

Genetics

Genotype and Phenotype Spectrum of *FRMD7*-Associated Infantile Nystagmus Syndrome

Jae-Hwan Choi,¹ Jae-Ho Jung,² Eun Hye Oh,¹ Jin-Hong Shin,¹ Hyang-Sook Kim,¹ Je Hyun Seo,² Seo Young Choi,³ Min-Ji Kim,³ Hee Young Choi,⁴ Changwook Lee,⁵ and Kwang-Dong Choi³

¹Department of Neurology, Pusan National University School of Medicine, Research Institute for Convergence of Biomedical Science and Technology, Pusan National University Yangsan Hospital, Yangsan, South Korea

²Department of Ophthalmology, Pusan National University School of Medicine, Research Institute for Convergence of Biomedical Science and Technology, Pusan National University Yangsan Hospital, Yangsan, South Korea

³Department of Neurology, Pusan National University Hospital, Pusan National University School of Medicine and Biomedical Research Institute, Busan, South Korea

⁴Department of Ophthalmology, Pusan National University Hospital, Pusan National University School of Medicine and Biomedical Research Institute, Busan, South Korea

⁵Department of Biological Sciences, School of Life Sciences, Ulsan National Institute of Sciences and Technology, Ulsan, South Korea

Correspondence: Kwang-Dong Choi, Department of Neurology, College of Medicine, Pusan National University Hospital 1-10 Ami-dong, Seo-gu, Busan 602-739, Korea; kdchoi@pusan.ac.kr

J-HC and J-HJ contributed equally to the work presented here and should therefore be regarded as equivalent authors.

Submitted: February 27, 2018

Accepted: May 28, 2018

Citation: Choi J-H, Jung J-H, Oh EH, et al. Genotype and phenotype spectrum of *FRMD7*-associated infantile nystagmus syndrome. *Invest Ophthalmol Vis Sci*. 2018;59:3181-3188. <https://doi.org/10.1167/iovs.18-24207>

PURPOSE. We investigate the genotype and phenotype spectrum of *FRMD7*-associated infantile nystagmus syndrome in Korean probands.

METHODS. A total of 37 patients with infantile nystagmus syndrome were recruited prospectively for genetic analysis. We performed polymerase chain reaction (PCR)-based direct sequencing and haplotype analysis for *FRMD7*. Detailed ophthalmic examinations and eye movement recordings were compared between *FRMD7* and non-*FRMD7* groups.

RESULTS. In 13 (35%) of 37 patients, five different mutations of *FRMD7* were detected: start codon mutation c.1A>G, splice site mutation c.162+6T>C, and three missense mutations (c.575A>C, c.722A>G, and c.875T>C). The latter mutation was identified in seven unrelated patients, and always was accompanied with two single nucleotide polymorphisms of exon 12 (rs6637934, rs5977623). Compared to non-*FRMD7* groups, a cup-to-disc ratio was significantly decreased in *FRMD7* groups ($P < 0.001$), and a disc-macula distance to disc diameter ratio markedly increased in the *FRMD7* group ($P = 0.015$). Most patients in the *FRMD7* group had at least two types of the nystagmus waveforms, and the most common type was unidirectional jerk nystagmus (75%), such as pure jerk and jerk with extended foveation, followed by pendular (25%), bidirectional jerk (19%), and dual jerk (6%) nystagmus. No significant differences were observed between *FRMD7* and non-*FRMD7* groups in terms of the nystagmus waveform, presence of periodic alternating nystagmus, and mean foveation time.

CONCLUSIONS. We identified five *FRMD7* mutations in 35% of our infantile nystagmus syndrome cohort, expanding its mutational spectrum. The missense mutation c.875T>C may be a common mutation arisen from the founder effect in Korea. Optic nerve dysplasia associated with *FRMD7* mutations suggests that the abnormal development of afferent visual systems may affect neural circuitry within the oculomotor system.

Keywords: infantile nystagmus syndrome, *FRMD7*, founder effect, optic nerve head dysplasia

Infantile nystagmus syndrome (INS) is characterized by involuntary oscillation of the eyes, which is present at birth or manifesting within the first few months of life.¹ It can be associated with visual system disorders, such as albinism, achromatopsia, and Leber congenital amaurosis, suggesting that the nystagmus may be sensory in origin. On the other hand, idiopathic IN (IIN) arises independently of any ocular or neurologic abnormalities. This has led to speculation that IIN may be caused by abnormal development of the ocular motor system itself rather than the afferent visual pathway.^{2,3}

INS is a genetically heterogeneous disorder. To date, more than 100 genes have been associated with INS and there is significant overlap in phenotypic characteristics.³⁻⁵ IIN may be inherited as an autosomal dominant, autosomal recessive, or X-

linked trait.⁶ The most common form of inheritance is X-linked, which can be dominant or recessive. Three X-linked loci have been reported at Xp11.4-p.11.3, Xp22, and Xq26-q27. In 2006, Tarpey et al.⁷ first identified pathogenic mutations in *FRMD7* located at Xq26. Approximately 50% of families with IIN have been linked to the *FRMD7* locus. Many studies revealed that *FRMD7* protein is expressed mainly in the developing ocular motor structures, such as the cerebellum and vestibular nucleus, and has an important role in control of eye movement and gaze stability.⁷⁻⁹ However, recent studies using optical coherence tomography (OCT) demonstrated that individuals with *FRMD7* mutations had abnormal retinal developments, including foveal hypoplasia and optic nerve head abnormalities.¹⁰ These raise a possibility that arrested retinal develop-



ments may be the underlying etiology in the development of nystagmus in IIN.

We performed molecular genetic analysis on *FRMD7* in a Korean cohort with INS to identify the causative mutations. We also investigated the ophthalmic and oculomotor characteristics of patients with *FRMD7* mutations to elucidate the phenotype of *FRMD7*-associated INS.

METHODS

Patients

We prospectively recruited 37 unrelated Korean patients (19 men, 18 women, age range 9–67 years, mean \pm SD = 33.5 \pm 15 years) with INS from the Neuro-ophthalmology Clinic of two university hospitals in Korea. INS was defined as conjugate oscillations of the eyes with onset within the first 6 months of life.¹ Other congenital forms of nystagmus, such as fusional maldevelopment nystagmus syndrome and spasmus nutans syndrome, were excluded. Of the patients, 13 had a family history of INS, and the remaining 24 were sporadic cases.

All experiments followed the tenets of the Declaration of Helsinki, and informed consent was obtained after the nature and possible consequences of this study had been explained to the participants. This study was approved by the institutional review boards of two participating hospitals (Pusan National University Hospital [PNUH] and Pusan National University Yangsan Hospital [PNUYH]). Because our study included all consecutive patients during the research period, two previously reported families were included in this report.¹¹

Clinical Assessments

A total of 41 patients, including four affected members within the family, received detailed ophthalmic examinations and eye movement recording. The ophthalmic examinations included best-corrected visual acuity (BCVA), color vision, and anterior segment observation with slit-lamp biomicroscopy. Visual acuity was measured using the Snellen chart and converted to logMAR for subsequent analysis. We evaluated color vision through Ishihara testing. Optic nerve dysplasia was assessed by morphologic analysis of the optic nerve head, including peripapillary pigment and double ring sign from fundus photographs. We also measured the cup-to-disc ratio (C/D ratio) and the disc-macula distance to disc diameter ratio (DM:DD ratio) as previously described.^{12,13} When the DM:DD ratio was greater than 3.0, small optic disc could be suspected.^{12,13}

Eye movements were recorded binocularly using infrared video-oculography (SLMED, Seoul, Korea). Spontaneous nystagmus was analyzed with and without fixation while the subjects attempted to look straight ahead. Types of waveforms were classified based on the 12 waveforms described by Dell'Osso and Daroff.¹⁴ In this study, we included patients with oculo-graphically diagnosed INS that exhibited distinctive waveforms, including increasing exponential slow phases or pendular type. Foveation time was measured from at least 40 beats of nystagmus as previously described, which was defined as a relatively constant eye position that occurred during an oscillatory cycle and lasted for at least 40 ms.^{15,16} Periodic alternating nystagmus (PAN) was identified from prolonged periods of recording over at least 10 minutes. Cycle duration and presence of periodicity were evaluated based on the previous report.¹⁷ We also evaluated the effects of convergence.

Mutation Analysis

We screened mutations in *FRMD7* by direct sequence analysis using genomic DNA from peripheral blood of the patients. All

coding exons and intron–exon junctions from *FRMD7* were amplified through polymerase chain reaction (PCR) with the primers listed in a previous study.¹¹ PCR-amplified products were separated and purified using 2% agarose gel and a DNA extraction kit (SolGent, Daejeon, Korea), cycle-sequenced with PCR primers using the BigDye Terminator Sequencing Kit (Applied Biosystems, Foster, CA, USA), and electrophoresed using an ABI PRISM 3730XL DNA analyzer (Applied Biosystems). We manually examined sequences for variants using Chromas software. The reference cDNA sequence was obtained from the Genbank database (NM_194277.1), when c.1 corresponds to the first nucleotide of the translation initiation codon. The variant was tested for novelty through searches of literature and public variant database, including the Human Gene Mutation Database (HGMD), Korean Personal Genome Project (KPGP) information, dbSNP147, the Exome Aggregation Consortium (ExAC), and the 1000 Genomes Project. Pathogenicity of nonsynonymous variants was analyzed using the following predictive software: SIFT (J. Craig Venter Institute; <http://sift.jcvi.org/>), PROVEAN (J. Craig Venter Institute; <http://provean.jcvi.org/>), and Mutation Taster (Charité Universitätsmedizin Berlin; <http://mutationtaster.org/>). We evaluated conservation at the base position using PhastCons (available in the public domain, <http://compugen.cshl.edu/phast/>). The variants were evaluated further in 150 normal controls using PCR and restriction fragment length polymorphism (PCR-RFLP) analysis.

Haplotype Analysis

To determine whether *FRMD7* mutations represent a founder effect, we performed haplotype analysis using the Axiom SNP array. Briefly, purified genomic DNA of the patients was amplified and fragmented. Then, a single-strand DNA fragment by denaturation was transferred to the HT hybridization Tray and loaded on the Axiom GeneTitan (Affymetrix, Santa Clara, CA, USA). The Hybridization Tray and the Custom 96 array plate moved to the Axiom GeneTitan were combined and reacted for 23 hours 30 minutes at a uniform temperature and then stained. Allele calling was performed using generated 'CEL files' with Axiom Analysis Suite (1.1.0.616). Axiom best practice workflow was followed to obtain high-quality genotyping results (available in the public domain at https://biobank.ctsu.ox.ac.uk/crystal/docs/axiom_genome_analguide.pdf). Samples with DQC < 0.82 and QC call rate < 97% were not considered for further analysis. PED/MAP files were generated after QC. We used 26 intragenic single nucleotide polymorphisms (SNPs) located in coding region or introns of *FRMD7* (See Supplementary Table S1), and conducted linkage disequilibrium (LD) block analysis using markers with minor allele frequency (MAF) > 0.01.

Molecular Structural Modeling of Missense Mutations

Structural modeling of wild type and mutants of human *FRMD7* FERM domain comprising residues 1 to 282 was performed using I-TASSER. The crystal structure of FERM domain of human protein DAL-1 (PDB accession code: 2HE7) having 40% sequence identity was used as a template. The resultant PDB files were visualized by Pymol (available in the public domain at www.pymol.org).

Statistical Analysis

A Mann-Whitney *U* test was used to compare continuous variables (visual acuity, C/D ratio, DM:DD ratio, mean foveation time of nystagmus) between *FRMD7* and non-*FRMD7* groups.

TABLE 1. *FRMD7* Mutations Identified in Patients With INS

Mutation	Protein Change	Exon/Intron	Variant Effect	In Silico Prediction					PhastCons	MA	Domain Affected	Patient ID	Mutation State
				SIFT	PROVEAN	MutationTaster	Disease-causing	MA					
c.1A>G	p.M1V	Exon 1	Start codon mutation	Damaging	Neutral	Disease-causing	1	0	FERM	F1	III2	heterozygous	
c.162+6T>C	-	Intron 2	Splice site mutation	-	-	-	-	0	FERM 1	F2	III1 III1 III2	hemizygous hemizygous heterozygous	
c.575A>C	p.H192P	Exon 7	Missense mutation	Damaging	Deleterious	Disease-causing	1	0	FERM 3	F3	III1 II5	heterozygous heterozygous	
c.722A>G	p.K241R	Exon 8	Missense mutation	Damaging	Deleterious	Disease-causing	1	0	FERM 3	F4	III2	hemizygous	
c.875T>C	p.L292P	Exon 9	Missense mutation	Damaging	Deleterious	Disease-causing	0.972	0.0003* 0.00003†	FA	S20 F4	III6	heterozygous heterozygous	
										S2 S3 S4 S9		hemizygous hemizygous hemizygous heterozygous	
										S10 S15		heterozygous heterozygous	

* MAF based on the 1000 Genomes Project.

† MAF based on the exome aggregation consortium (ExAC).

Categorical variables were compared using the Pearson's χ^2 test or Fisher's exact test between two groups.

RESULTS

Molecular Genetic Results

The patient's molecular findings are summarized in Table 1 and Figure 1A. Five different mutations were detected in 13 (35%) of 37 unrelated patients. Six patients had a family history of INS (Fig. 2). Four mutations were novel: start codon mutation c.1A>G (p.M1V), splice site mutation c.162+6T>C, and two missense mutations c.575A>C (p.H192P) and c.722A>G (p.K241R). The remaining one was reported previously: missense mutation c.875T>C (p.L292P).¹⁸ All mutations were not found in 150 healthy controls.

We detected c.1A>G of exon 1 in two unrelated families (F1 and 2). The mutation leads to loss of the primary start codon ATG for methionine, which is replaced by a triplet GTG for valine. The alternative in-frame start codon is not present around a mutation. This mutation also was detected in another affected member within each family. In F3, a splice-site mutation was found at the 6th nucleotide of the splice donor site on intron 2 (c.162+6T>C). The mutation also was detected in proband's mother and absent in public databases. Human Splicing Finder (HSF) predicted that this mutation will break the splice site and make new splice sites resulting in four bases longer on exon 2. A missense mutation c.575A>C of exon 7 was identified in two unrelated families (F5 and 6). The mutation would result in amino acid substitution of histidine by proline at codon 192. Another missense mutation was c.722A>G of exon 8 in a sporadic case (S20), which changed a highly conserved amino acid lysine by glycine at codon 241. Both missense mutations were absent in public databases and predicted to be pathogenic by all three prediction tools. The last mutation was the known missense mutation c.875T>C, which was found in a Belgian family with IIN.¹⁸ In our cohort, this mutation was detected in seven patients, including one family (F4) and six sporadic cases (S2, S3, S4, S9, S10, and S15). It had a MAF of 0.0003 in the 1000 Genomes Project and 0.00003 in the ExAC Browser, but was absent in in-house controls. It was predicted to be pathogenic by all prediction tools, and the mutated residue of leucine was highly conserved.

Haplotype analysis was performed in seven unrelated patients with the c.875T>C mutation (See Supplementary Table S1). In SNPs analysis, we could not establish any LD among the SNPs within *FRMD7*. Furthermore, the 5000 kb region around *FRMD7* showed no LD. However, direct sequence analysis of *FRMD7* revealed that the c.875T>C mutation always was observed with two SNPs of exon 12, including c.1403G>A (rs6637934, MAF = 0.066) and c.1533T>C (rs5977623, MAF = 0.259; Fig. 1A). These SNPs were not observed in patients with another *FRMD7* mutations except for c.162+6T>C (Table 2).

Protein Structural Modeling

Figure 1B shows the structural modeling of novel missense mutations (p.H192P and p.K241R). The H192 residue is located in the middle of the β -sheets within F3-FERM domain. Therefore, the p.H192P mutation is likely to destabilize the overall structure of *FRMD7* by disrupting the core β -strand conformation. On the other hand, the effect caused by the p.K241R mutation is not clearly apparent because it is located at the end of the predicted β -strand. Moreover, the side chain of lysine (K) is structurally similar to that of arginine (R),

TABLE 2. Patterns of Two SNPs in Patients With *FRMD7* Mutations

Pathogenic Mutations	Patient ID	rs6637934 (c.1403G>A)	rs5977623 (c.1533T>C)
c.1A>G, p.M1V	F1	GG	TT
	F2	GG	TT
c.162+6T>C	F3	A (hemizygous)	C (hemizygous)
	F5	G (hemizygous)	T (hemizygous)
c.575A>C, p.H192P	F6	G (hemizygous)	T (hemizygous)
	S20	G (hemizygous)	T (hemizygous)
c.722A>G, p.K241R	F4	G/A (heterozygous)	T/C (heterozygous)
	S2	A (hemizygous)	C (hemizygous)
c.875T>C, p.L292P	S3	A (hemizygous)	C (hemizygous)
	S4	A (hemizygous)	C (hemizygous)
	S9	G/A (heterozygous)	T/C (heterozygous)
	S10	G/A (heterozygous)	T/C (heterozygous)
	S15	A (hemizygous)	C (hemizygous)

suggesting that the mutation from lysine to arginine in this residue might not significantly affect overall structure.

Clinical Characteristics

Detailed ophthalmic and oculomotor findings of patients with *FRMD7* mutations are summarized in Supplementary Tables S2 and S3. Comparisons of clinical characteristics between patients with and without *FRMD7* mutations are described in Table 3. In the *FRMD7* group, the mean C/D ratio was below normal range (0.33 ± 0.15 , normal $0.4\sim 0.6$), and significantly decreased compared to that in the non-*FRMD7* group (0.51 ± 0.20 , $P < 0.001$; Fig. 3), whereas the mean DM:DD ratio considerably increased in the *FRMD7* group (3.04 ± 0.53) compared to the non-*FRMD7* group (2.80 ± 0.37 , $P = 0.015$). Four patients in the *FRMD7* group had morphologic changes of

the optic nerve head, including segmental hypoplasia (III1 of F1 and III6 of F4) and peripapillary pigment (S15 and S20). None of the *FRMD7* group patients had macular hypoplasia or anomalies of anterior segments. The *FRMD7* group had a better visual acuity than the non-*FRMD7* group, but there were no significant differences in color vision abnormalities and presence of strabismus between the groups.

The waveforms of nystagmus were classified into the 12 categories of pendular, jerk (uni- and bidirectional), and dual jerk waveforms. Most patients in the *FRMD7* group had at least two types of waveforms. The most common type was unidirectional jerk nystagmus (75%), such as pure jerk and jerk with extended foveation, followed by pendular (25%), bidirectional jerk (19%), and dual jerk (6%) nystagmus. Two patients in the *FRMD7* group had a PAN with a periodic (S2) or an aperiodic (S4) cycle. Foveation time ranged from 59 to 158 ms (mean \pm SD = 100 ± 30 ms) in the *FRMD7* group. No significant differences were observed between the *FRMD7* and non-*FRMD7* groups in terms of waveform of nystagmus (Fig. 4), presence of PAN, mean foveation time, nystagmus changes in darkness, and convergence effect for the nystagmus.

DISCUSSION

We identified five *FRMD7* mutations in 35% (13/37) of our total INS cohort. Four of them were novel mutations. Interestingly, some unrelated patients had the same mutation, and the known mutation of p.L292P was found in 54% (7/13) of the *FRMD7* group. In addition, the mutation detection rate of sporadic cases (7/24, 29%) was higher than that in other studies. Our study supported that *FRMD7* mutations are the underlying pathogenesis of the molecular mechanism for INS.

The *FRMD7* consists of 12 exons and encodes a 714-residue polypeptide.^{6,19} It contains a conserved N-terminal FERM domain and FERM-adjacent (FA) domain, whereas the C-terminal region has no significant homology to other pro-

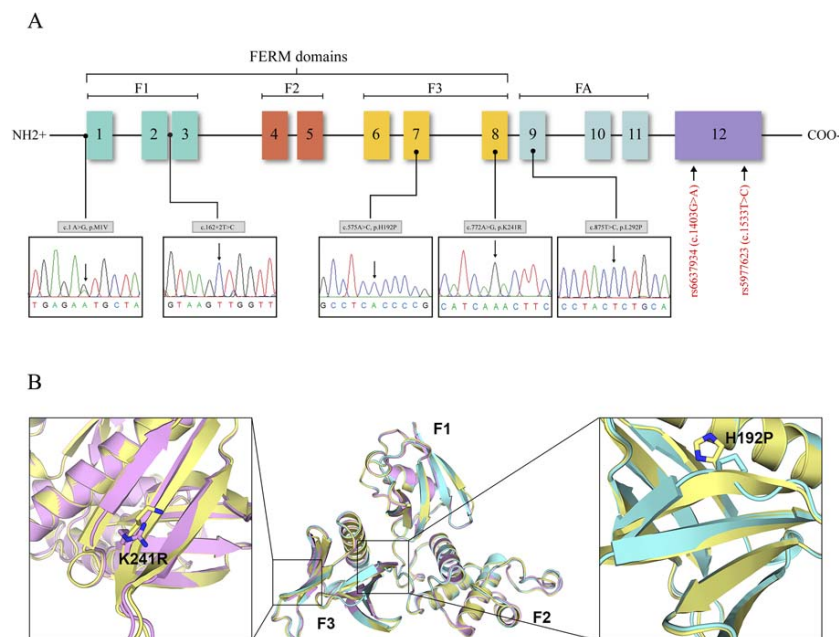


FIGURE 1. Localization of *FRMD7* mutations and protein structural modeling of two novel mutations. (A) The *FRMD7* contains an N-terminal FERM domain (F1, F2, and F3 lobes) and FERM-adjacent (FA) domain. The positions of the mutations are indicated at the bottom of the Figure (arrow). All patients carrying the c.875T>C mutation share two SNPs (c.1403G>A, rs6637934; c.1533T>C, rs5977623) of exon 12 within *FRMD7*. (B) The ribbon diagram shows a superposition of structural model of the FERM domains of *FRMD7* of wild type (yellow), K241R (pink), and H192P (cyan) mutants.

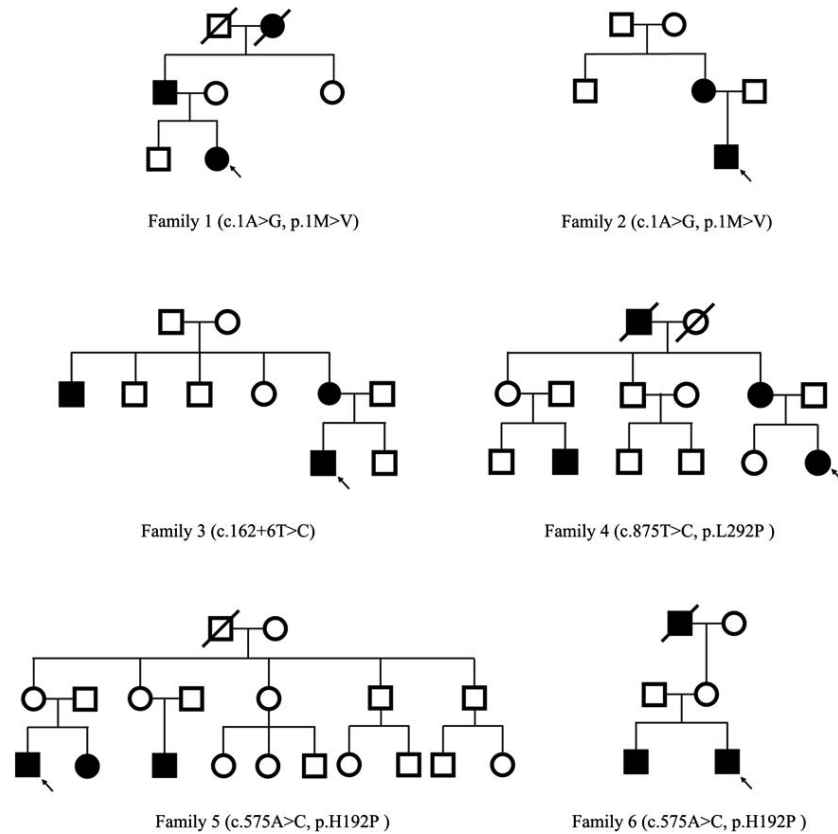


FIGURE 2. Pedigree of six patients with *FRMD7* mutations who had a family history of INS.

teins.¹⁹ The *FRMD7* protein is expressed in the developing brain, which control eye movements and gaze stability, and has been shown to involve regulation of neuronal cytoskeletal dynamics through CASK-induced or Rho GTPase signaling.^{4,20–23} Thus, *FRMD7* mutations can cause abnormal eye movements and gaze instability. To date, over 70 different mutations within *FRMD7* have been reported.^{5,7,9–11,18,19,24–27} Many mutations cluster around the F3 lobes of the FERM and

FA domains. This suggests that these domains have important roles in the function of *FRMD7*. Three (p.H192P, p.K241R, and p.L292P) of our mutations are located in the F3 lobe and FA domain. The molecular structural modeling reveals that p.H192P mutation is likely to destabilize the overall structure of *FRMD7* protein by disrupting the core β -strand conformation, but the effect of p.K241R mutation is not clearly apparent. Previously, p.L292P mutation, which is located in

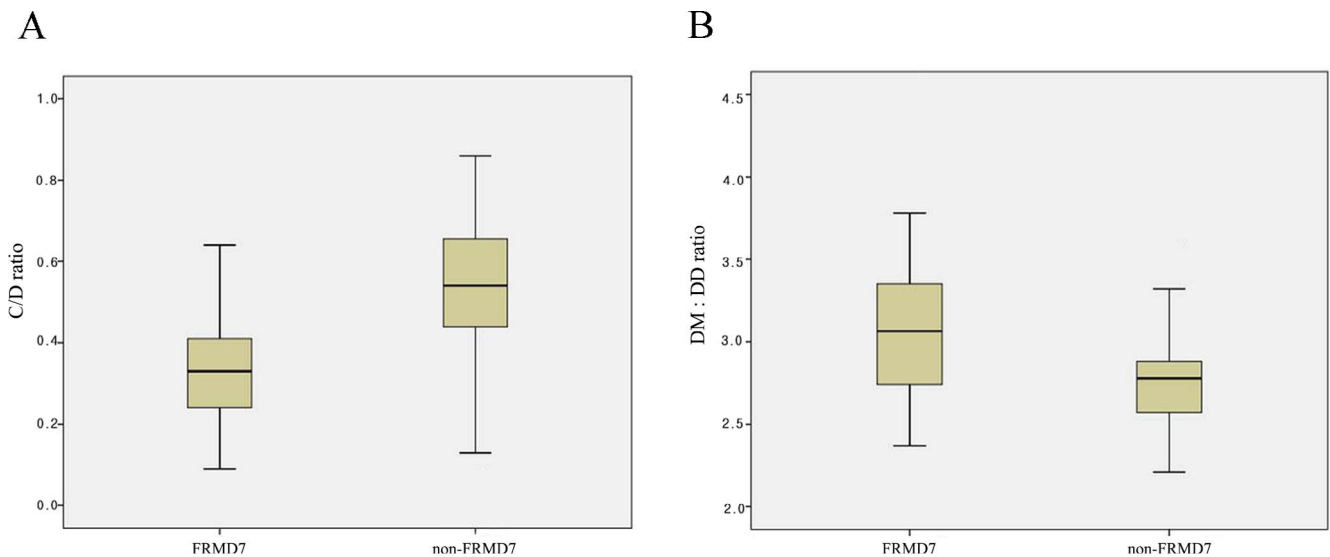


FIGURE 3. C/D and DM:DD ratio of the patients. Mean C/D (A) and DM:DD (B) ratios are significantly different between the *FRMD7* and non-*FRMD7* groups.

TABLE 3. Comparisons of Clinical Characteristics Between *FRMD7* and Non-*FRMD7* Groups

	<i>FRMD7</i> group, n = 16	Non- <i>FRMD7</i> group, n = 25	P Value
Sex, male, n (%)	10 (63)	13 (52)	0.453
Visual acuity, logMAR			
Right eye	+0.25	+0.75	0.051
Left eye	+0.21	+0.67	0.006
Color vision abnormality, n (%)	1 (7)	2 (10)	0.773
Strabismus, n (%)	2 (15)	4 (18)	1.000
Anomaly of anterior segment, n (%)	0 (0)	8 (33)	0.015
Macular hypoplasia, n (%)	0 (0)	6 (29)	0.041
C/D ratio, mean ± SD	0.33 ± 0.15	0.51 ± 0.20	<0.001
DM:DD ratio, mean ± SD	3.04 ± 0.53	2.80 ± 0.37	0.015
Waveform of nystagmus, n (%)			
Pendular	4 (25)	7 (28)	0.564
Unidirectional jerk	12 (75)	23 (92)	0.147
Bidirectional jerk	3 (19)	4 (16)	0.569
Dual jerk	1 (6)	1 (4)	0.634
PAN, n (%)	2 (16)	7 (25)	0.441
Foveation time of nystagmus, mean ± SD (ms)	100 ± 30	108 ± 39	0.429
Nystagmus change in darkness, n (%)			
Augmentation	0 (0)	4 (20)	0.124
Suppression	6 (38)	8 (40)	0.832
No change	6 (38)	7 (35)	0.943
Directional change	4 (25)	1 (5)	0.141
Nystagmus change during convergence, n (%)			
Augmentation	2 (13)	0 (0)	0.483
Suppression	9 (60)	8 (62)	0.713
No change	3 (20)	4 (31)	0.427

the FA domain was predicted to lead to change in α -helix conformation of the FA domain due to lack of a hydrogen on the amino group of proline and can also affect the recognition specificity of the hydrophobic ligands.¹⁸ However, these structural predictions must be verified using X-ray crystallography.

Among our mutations, the p.L292P mutation accounted for more than 50% of total patients with *FRMD7* mutations. All patients carrying the p.L292P mutation came from the same restricted region (Gyeongsangnam-do) of Korea and shared common SNPs (rs6637934, rs5977623) of exon 12 within *FRMD7*. c.1403G>A (rs6637934) of two SNPs is a relatively rare variant with a MAF of 0.066, and also has been detected in another Korean INS family with the p.L292P mutation.²⁸ These findings suggest that the p.L292P mutation might have arisen from the founder effect. The size of the shared haplotype may be small, because SNP analysis did not show LD around *FRMD7*. Historically, Gyeongsangnam-do, which is located in the southeast region of Korea, had been a part of the Silla of Three Kingdoms period in ancient times. In this region, a population mixing with neighboring populations was not easy due to geographic position, and there is a distinctive dialect and lifestyle. The fact that other mutations (p.M1V and p.H192P) also were detected in two unrelated families supports this explanation.

FRMD7 mutation is known to be linked to idiopathic INS without any abnormalities in visual systems. Our patients with *FRMD7* mutations also showed relatively good vision without

anomalies of anterior segments and macular hypoplasia. This leads to the assumption that *FRMD7* mutations cause a primary defect in regions of the brain responsible for ocular motor control. However, the *FRMD7* group in our study had a small C/D ratio and high DM:DD ratio, suggesting morphologic changes within the optic nerve head.^{12,13} Previous studies with OCT revealed retinal and optic nerve changes, including a shallow foveal pit, increased central macular thickness, decreased peripapillary retinal nerve fiber layer thickness, and shallow optic nerve cup in IIN patients with *FRMD7* mutations.^{10,29} They demonstrated *FRMD7* mRNA expressions in the developing human retina and optic disc. We also reported anomalous appearances of the optic nerve head using OCT in patients with *FRMD7* mutations.¹¹ Recently, *FRMD7* expression has been localized in starburst cells of the retina to establish spatially asymmetric inhibitory inputs to direction-selective ganglion cells (DS cells) along the horizontal axis.³⁰ The dysfunction of *FRMD7* might contribute to the lack of the horizontal optokinetic reflex by loss of horizontal direction selectivity. These findings reflect that the abnormal development of afferent visual systems may be associated with *FRMD7* mutations and could affect neural circuitry within the oculomotor system.

Few studies have systematically investigated the nystagmus pattern of patients with *FRMD7* mutations.³¹⁻³³ In our *FRMD7* group, unidirectional jerk nystagmus was the most common waveform, while pendular nystagmus was less common (25%) than in previous reports (approximately 45%).^{31,32} There was intra- and interfamilial variability in the nystagmus waveforms, and the phenotypes were not affected by the type of mutation. Although PAN was observed in two patients with the p.L292P mutation, another patient with the same mutation had no PAN. Previously, idiopathic infantile PAN associated with other *FRMD7* mutations has been reported.³³ These findings are in accordance with those of previous reports supporting the phenotypic variability of *FRMD7* mutations.³¹⁻³³ Furthermore, we could find no difference in nystagmus characteristics between patients with and without *FRMD7* mutations. This implied the complex mechanisms to generate various waveforms associated with INS, which include abnormal neural circuitry of the slow eye movement and gaze-holding systems.³⁴⁻³⁶ This could be explained by the effect of other modifier genes or environmental factors. Alternatively, *FRMD7* mutation alone is insufficient to generate nystagmus, but cerebellar plasticity may amplify and shape nystagmus waveforms similar to the hypothesis of oculopalatal tremor.^{4,37} The learning process in the cerebellum can be variable and diverse among individuals. Indeed, a previous study using a functional MRI identified the decline of the cerebellum as a possible site of the ocular motor network involved in INS.³⁸

This study has potential limitations. We did not check the binocular visual acuity. It would be more likely to represent the BCVA than monocular visual acuity in patients with nystagmus. Furthermore, we did not perform quantitative approaches of foveal hypoplasia and optic nerve changes using OCT imaging. The quantitative OCT measurements can achieve analysis of afferent visual systems in much greater detail than fundus photography.

In conclusion, we identified five *FRMD7* mutations in our INS cohort. In particular, the missense mutation c.875T>C may be a common mutation arisen from the founder effect in Korea. Our results expand the mutation spectrum of *FRMD7* and provide molecular evidence for the underlying pathogenesis of INS. Optic nerve dysplasia associated with *FRMD7* mutations suggested that the abnormal development of afferent visual systems may affect neural circuitry within the oculomotor system.

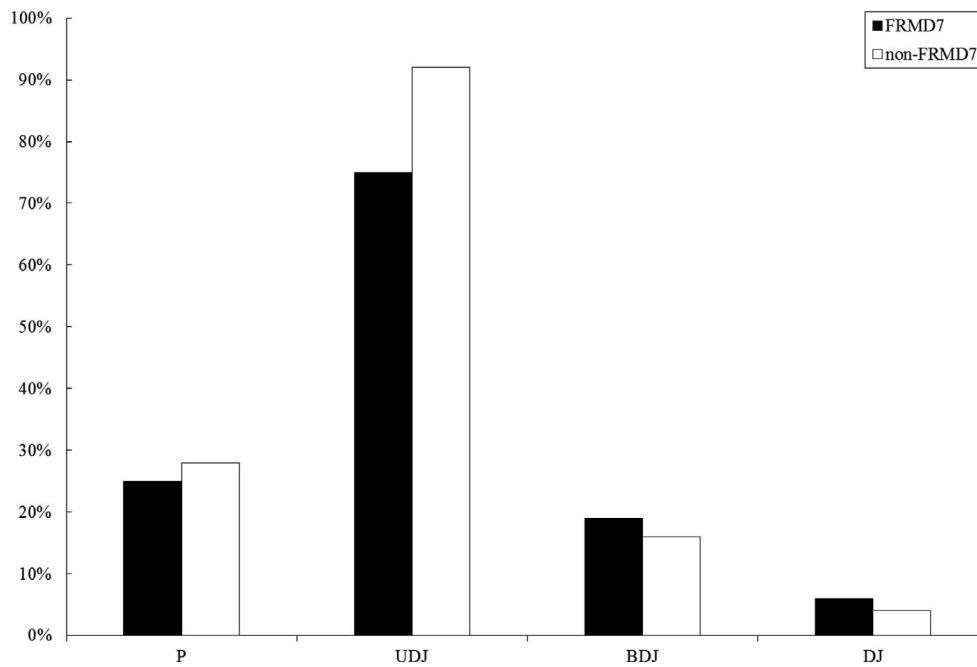


FIGURE 4. Waveforms of the nystagmus. There are no significant differences in waveforms of nystagmus between the *FRMD7* and non-*FRMD7* groups. P, pendular; UDJ, unidirectional jerk; BDJ, bidirectional jerk; DJ, dual jerk.

Acknowledgments

The authors thank all patients who participated in this study.

Supported by Basic Science Research Program through the National Research Foundation of Korea funded by the Ministry of Education (NRF-2017R1D1A3B03033237).

Disclosure: **J.-H. Choi**, None; **J.-H. Jung**, None; **E.H. Oh**, None; **J.-H. Shin**, None; **H.-S. Kim**, None; **J.H. Seo**, None; **S.Y. Choi**, None; **M.-J. Kim**, None; **H.Y. Choi**, None; **C. Lee**, None; **K.-D. Choi**, None

References

- Leigh RJ, Zee DS. *The Neurology of Eye Movements*. 5th ed, New York: Oxford University Press; 2015.
- Brodsky MC, Dell'Osso LE. A unifying neurologic mechanism for infantile nystagmus. *JAMA Ophthalmol*. 2014;132:761-768.
- Richards MD, Wong A. Infantile nystagmus syndrome: clinical characteristics, current theories of pathogenesis, diagnosis, and management. *Can J Ophthalmol*. 2015;50:400-408.
- Gottlob I, Proudlock FA. Aetiology of infantile nystagmus. *Curr Opin Neurol*. 2014;27:83-91.
- Rim JH, Lee ST, Gee HY, et al. Accuracy of next-generation sequencing for molecular diagnosis in patients with infantile nystagmus syndrome. *JAMA Ophthalmol*. 2017;135:1376-1385.
- Self J, Lotery A. A review of the molecular genetics of congenital idiopathic nystagmus (CIN). *Ophthalmic Genet*. 2007;28:187-191.
- Tarpey P, Thomas S, Sarvananthan N, et al. Mutations in *FRMD7*, a newly identified member of the FERM family, cause X-linked idiopathic congenital nystagmus. *Nat Genet*. 2006;38:1242-1244.
- Self J, Haitchi HM, Griffiths H, Holgate ST, Davies DE, Lotery A. *Frmd7* expression in developing mouse brain. *Eye*. 2010;24:165-169.
- Thomas MG, Crosier M, Lindsay S, et al. The clinical and molecular genetic features of idiopathic infantile periodic alternating nystagmus. *Brain*. 2011;134:892-902.
- Thomas MG, Crosier M, Lindsay S, et al. Abnormal retinal development associated with *FRMD7* mutations. *Hum Mol Genet*. 2014;23:4086-4093.
- Choi JH, Shin JH, Seo JH, Jung JH, Choi KD. A start codon mutation of the *FRMD7* gene in two Korean families with idiopathic infantile nystagmus. *Sci Rep*. 2015;5:13003.
- Wakakura M, Alvarez E. A simple clinical method of assessing patients with optic nerve hypoplasia. The disc-macula distance to disc diameter ratio (DM/DD). *Acta Ophthalmol (Copenh)*. 1987;65:612-617.
- Alvarez E, Wakakura M, Khan Z, Dutton GN. The disc-macula distance to disc diameter ratio: a new test for confirming optic nerve hypoplasia in young children. *J Pediatr Ophthalmol Strabismus*. 1988;25:151-154.
- Dell'Osso LE, Daroff RB. Congenital nystagmus waveforms and foveation strategy. *Doc Ophthalmol*. 1975;39:155-182.
- Hertle RW, Maldonado VK, Maybodi M, Yang D. Clinical and ocular motor analysis of the infantile nystagmus syndrome in the first 6 months of life. *Br J Ophthalmol*. 2002;86:670-675.
- Felius J, Fu VL, Birch EE, Hertle RW, Jost RM, Subramanian V. Quantifying nystagmus in infants and young children: relation between foveation and visual acuity deficit. *Invest Ophthalmol Vis Sci*. 2011;52:8724-8731.
- Hertle RW, Reznick L, Yang D. Infantile aperiodic alternating nystagmus. *J Pediatr Ophthalmol Strabismus*. 2009;46:93-103.
- AlMoallem B, Bauwens M, Walraedt S, et al. Novel *FRMD7* mutations and genomic rearrangement expand the molecular pathogenesis of x-linked idiopathic infantile nystagmus. *Invest Ophthalmol Vis Sci*. 2015;56:1701-1710.
- Watkins RJ, Thomas MG, Talbot CJ, Gottlob I, Shackleton S. The Role of *FRMD7* in idiopathic infantile nystagmus. *J Ophthalmol*. 2012;2012:460956.

20. Wakkins RJ, Patil R, Goult BT, Thomas MG, Gottlob I, Shackleton S. A novel interaction between FRMD7 and CASK: evidence for a causal role in idiopathic infantile nystagmus. *Hum Mol Genet* 2013;22:2105–2018.
21. Pu J, Mao Y, Lei X, et al. FERM domain containing protein 7 interacts with the Rho GDP dissociation inhibitor and specifically activates Rac1 signaling. *PLoS One*. 2013;8:e73108.
22. Betts-Henderson J, Bartesaghi S, Crosier M, et al. The nystagmus-associated FRMD7 gene regulates neuronal outgrowth and development. *Hum Mol Genet*. 2010;19:342–351.
23. Pu J, Lu X, Zhao G, Yan Y, Tian J, Zhang B. FERM domain containing protein 7 (FRMD7) upregulates the expression of neuronal cytoskeletal proteins and promotes neurite outgrowth in Neuro-2a cells. *Mol Vis*. 2012;18:1428–1435.
24. Zhang X, Ge X, Yu Y, et al. Identification of three novel mutations in the FRMD7 gene for X-linked idiopathic congenital nystagmus. *Sci Rep*. 2014;4:3745.
25. Radhakrishna U, Ratnamala U, Deutsch S, et al. Novel homozygous, heterozygous and hemizygous FRMD7 gene mutations segregated in the same consanguineous family with congenital X-linked nystagmus. *Eur J Hum Genet*. 2012;20:1032–1036.
26. Guo Y, Song Z, Xu H, et al. Heterogeneous phenotype in a family with the FERM domain-containing 7 gene R335X mutation. *Can J Ophthalmol*. 2014;49:50–53.
27. Thomas MG, Maconachie G, Sheth V, McLean RJ, Gottlob I. Development and clinical utility of a novel diagnostic nystagmus gene panel using targeted next-generation sequencing. *Eur J Hum Genet*. 2017;25:725–734.
28. Oh SY, Shin BS, Seo MW, Ki CS, Hwang JM, Kim JS. Novel Mutation in FRMD7 Gene in X-linked Congenital Nystagmus. *Res Vestib Sci*. 2007;6:155–160.
29. Thomas MG, Gottlob I. Optical coherence tomography studies provides new insights into diagnosis and prognosis of infantile nystagmus: a review. *Strabismus*. 2012;20:175–180.
30. Yonehara K, Fiscella M, Drinnenberg A, et al. Congenital nystagmus gene FRMD7 is necessary for establishing a neuronal circuit asymmetry for direction selectivity. *Neuron*. 201;89:177–193.
31. Thomas S, Proudlock FA, Sarvananthan N, et al. Phenotypical characteristics of idiopathic infantile nystagmus with and without mutations in FRMD7. *Brain*. 2008;131:1259–1267.
32. Kumar A, Gottlob I, McLean RJ, Thomas S, Thomas MG, Proudlock FA. Clinical and oculomotor characteristics of albinism compared to FRMD7 associated infantile nystagmus. *Invest Ophthalmol Vis Sci*. 2011;52:2306–2313.
33. Thomas MG, Crosier M, Lindsay S, et al. The clinical and molecular genetic features of idiopathic infantile periodic alternating nystagmus. *Brain*. 2011;134:892–902.
34. Dell'Osso LF, van der Steen J, Steinman RM, Collewijn H. Foveation dynamics in congenital nystagmus. I: Fixation. *Doc Ophthalmol*. 1992;79:1–23.
35. Dell'Osso LF, van der Steen J, Steinman RM, Collewijn H. Foveation dynamics in congenital nystagmus. II: Smooth pursuit. *Doc Ophthalmol*. 1992;79:25–49.
36. Dell'Osso LF, van der Steen J, Steinman RM, Collewijn H. Foveation dynamics in congenital nystagmus. III: Vestibulo-ocular reflex. *Doc Ophthalmol*. 1992;79:51–70.
37. Shaikh AG, Hong S, Liao K, et al. Oculopalatal tremor explained by a model of inferior olivary hypertrophy and cerebellar plasticity. *Brain*. 2010;133:923–940.
38. Leguire LE, Kashou NH, Fogt N, et al. Neural circuit involved in idiopathic infantile nystagmus syndrome based on FMRI. *J Pediatr Ophthalmol Strabismus*. 2011;48:347–356.